Molecular Crystals and Liquid Crystals Science and Technology. Section A. Molecular Crystals and Liquid Crystals

Publication details, including instructions for authors and subscription information:
http://www.tandfonline.com/loi/gmcl19

Guided Optical Waves in a Ferroelectric Liquid Crystal Layer: A Birefringence Analysis of Molecular Orientation on the Switching Process

S. Ito [a b], F. Kremer [a c], T. Fischer [d c] & W. Knoll [e]

[a] Max-Planck-Institut für Polymerforschung, Ackermannweg 10, D-55021, Mainz, Germany

[b] S. Ito is now with the Department of Polymer Chemistry, Kyoto University, Sakyo, Kyoto, 606, Japan

[c] F. Kremer and T. Fischer are now with FB Physik der Universität Leipzig, 04103, Leipzig, Germany

[d] Institut für Physik, Johannes Gutenberg Universität, Staudingerweg 7, D-55021, Mainz, Germany

[e] The Institute of Physical and Chemicai Research (RIKEN), Frontier Research Program, 2-1 Hirosawa, Wako, Saitama, 351-01, Japan

Version of record first published: 23 Sep 2006.

To cite this article: S. Ito , F. Kremer , T. Fischer & W. Knoll (1995): Guided Optical Waves in a Ferroelectric Liquid Crystal Layer: A Birefringence Analysis of Molecular Orientation on the Switching Process, Molecular Crystals and Liquid Crystals Science and Technology. Section A. Molecular Crystals and Liquid Crystals, 264:1, 99-114

To link to this article: http://dx.doi.org/10.1080/10587259508037305

Mol. Cryst. Liq. Cryst., 1995, Vol. 264, pp. 99–114
Reprints available directly from the publisher
Photocopying permitted by license only

Guided Optical Waves in a Ferroelectric Liquid Crystal Layer: A Birefringence Analysis of Molecular Orientation on the Switching Process

S. ITO[a] and F. KREMER[b]

Max-Planck-Institut für Polymerforschung, Ackermannweg 10, D-55021 Mainz, Germany

T. FISCHER[b]

Institut für Physik, Johannes Gutenberg Universität, Staudingerweg 7, D-55021 Mainz, Germany

W. KNOLL*

The Institute of Physical and Chemical Research (RIKEN), Frontier Research Program, 2-1 Hirosawa, Wako, Saitama 351-01, Japan

(Received April 29, 1994; in final form July 29, 1994)

Guided optical waves are very sensitive to the alteration of optical properties of dielectric media. In this report, we demonstrate the use of guided waves for studying dynamic behavior of ferroelectric liquid crystals. Propagating light in the anisotropic medium suffers a birefringent effect, which causes coupling of *p*- and *s*-polarized light. Theoretical calculations, based on the Maxwell equations, successfully describe this phenomena, using a dielectric tensor diagonal in molecular coordinates, which is transformed to the laboratory coordinate system by three Euler angles. The waveguide measurements are able to probe the molecular orientation and movement of the liquid crystal molecules in the three dimensional coordinate system. This method has been used to examine the switching behavior in the SmC* phase. The bistable states and the path of the molecular swing under alternating external electric fields are well characterized by the reflected intensity of single and double frequency modulation.

Keywords: Ferroelectric liquid crystals, molecular orientation, guided optical waves, birefringence

1. INTRODUCTION

Recently, guided optical waves have been utilized as a new analytical tool for the characterization of dielectric thin films and coatings.[1–3] The main advantage of this

[a] S. Ito is now with the Department of Polymer Chemistry, Kyoto University, Sakyo, Kyoto 606, Japan.
[b] F. Kremer and T. Fischer are now with FB Physik der Universität Leipzig, 04103 Leipzig, Germany.
* Author for correspondence

method is its sensitivity to small changes in optical properties. Thickness and refractive index changes in the sample modify the coupling conditions between the guided modes and the incident light. This effect is observed as a shift of the angle of incidence at the resonance condition, or as a large modulation of reflected intensity at a fixed angle.[4] Furthermore, guided light waves can be excited with both TM and TE modes, *i.e.* *p*-and *s*-polarized light. This offers a particular advantage in the study of anisotropic media, since both orientations of the electric field of the light are accessible with the same geometrical arrangement of the sample.[5,6]

From application standpoints, various electro-optic devices employing liquid crystals have been demonstrated. Among them, ferroelectric liquid crystals are promising materials, because of the strong interaction of the molecules with both light and external electric field.[7] Following the pioneering work of Meyer *et al.*[8] the peculiar characteristics of ferroelectric liquid crystals, e.g., the fast switching speed, the memory effect and the threshold behavior, have evoked extensive demand for such electro-optic devices.[9]

Guided optical waves have been used to study the optical properties of liquid crystals.[10] Sambles *et al.* have used this method to determine the molecular orientation and layer structure in a ferroelectric liquid crystal cell and demonstrated that this method provides extraordinary detail of the director profile in the cell.[11–16] We have applied the guided wave method to the study of switching behavior of ferroelectric liquid crystals, and have reported some initial results in a previous paper.[17] The appropriate choice of observation angles enables determination of the diagonal elements of the dielectric tensor, but more general treatments including birefringence effects on the guided waves are required in order to gain more detailed understanding of the dynamic behavior of liquid crystal molecules. Berreman introduced a 4×4 matrix technique to solve problems of reflection and transmission by anisotropic liquid crystal layers.[18] We have used this method with a somewhat different approach, and have tried to explain the switching behavior under an alternating electric field. This work is intended to demonstrate the utility of the guided wave method as a novel technique for the study of dynamic behavior of ferroelectric liquid crystals.

2. EXPERIMENTAL

2.1 Sample Preparation

A pure liquid crystalline sample, 4-(3-(S)-methyl-2-(S)-chloropentanoyloxy)-4′-octyloxy-biphenyl, having two chiral centers was used in the present study.[19,20] The phase transition temperatures are known to be:

Crys.-49°-SmC* - 55°-SmA-65°-Iso.

The sample preparation procedure has been described in detail in the previous report.[17] The liquid crystal was sandwiched between two glass plates whose surface was coated with gold metal and polyimide (Japan Synthetic Rubber Co.) layers. The

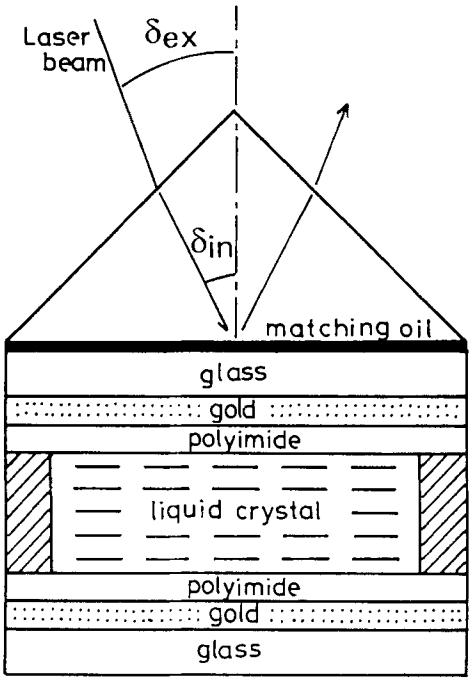

FIGURE 1 Schematic drawing of the liquid crystal cell used for guided wave measurements.

optical parameters of these layers were determined by surface plasmon measurements before making the sandwich cell. In order to obtain a uniform orientation of liquid crystal molecules, the polyimide surface was rubbed with a piece of soft cloth under an appropriate pressure. The thickness of the liquid crystal layer was 3–4 μm, and was determined by a polyester spacer film. The liquid crystal cell obtained has a symmetrical 7 layer configuration as shown in Figure 1. The top face of the cell was coupled to a prism using an index-matching oil, thus enabling us to choose a suitable plane of incidence for the light, by rotating the cell with respect to the prism.

2.2 Measurements

The sample was mounted on a temperature regulated brass holder, and set on a computer-controlled two-stage goniometer. A linearly polarized beam from a He-Ne laser, 5 mW at 632.8 nm, with the polarization being rotated by a $\lambda/2$ Fresnel Rhombus prism, is focussed on the prism with a beam diameter less than 0.1 mm. The *p*- and *s*-components of the reflected light were separately detected by a photodiode using a Glan-Thompson polarizer. An external electric field (E-field) was applied across the gold layers by a function generator (Kontron Elektronik, model Series 8201). The reflected intensities were recorded as a function of the angle of incidence using a lock-in amplifier (EG & G model 5208).

3. THEORY

The numerical calculation of the reflectivity determines the electric fields of the multilayer system, using a transfer matrix method similar to that of Berreman,[18] but using normal modes of the electric fields. The electric field inside each layer is described by the sum of four normal modes:

$$\mathbf{E}^n(x,z,t) = \sum_{\lambda=1}^{4} E_\lambda^n(z')\xi_\lambda^n e^{i(k_\parallel x + k_\perp^{n,\lambda}(z-z') - \omega t)} \tag{1}$$

with ω the frequency, and $k_\parallel$ the lateral momentum, independent of the layer and of the mode λ, $k_\perp^{n,\lambda}$ the momentum perpendicular to the layer interfaces and ξ_λ^n the polarization vectors ($\|\xi_\lambda^n\| = 1$) of layer n. Both $k_\perp^{n,\lambda}$ and ξ_λ^n differ from layer to layer and mode to mode and are given by the solution to the wave equation:

$$M(k_\perp^\lambda)_{i,j}\xi_{\lambda,j} = \left[\left(\frac{\omega}{c}\right)^2 \varepsilon_{i,j} + k_i^\lambda k_j^\lambda - (k^\lambda)^2\delta_{i,j}\right]\xi_{\lambda,j} = 0$$

$$k^\lambda = (k_\parallel, 0, k_\perp^\lambda)$$

with c the speed of light, $\varepsilon_{i,j}$, $(i,j = 1,\ldots,3)$ the dielectric tensor, and omitting the layer index n. The four values of $k_\perp^\lambda$, $\lambda = 1,\ldots,4$ are given by the four roots of the equation:

$$\det\left|\left(\frac{\omega}{c}\right)^2 \varepsilon_{i,j} + k_i^\lambda k_j^\lambda - (k^\lambda)^2\delta_{i,j}\right| = \sum_{m=0}^{4} c_m (k_\perp^\lambda)^m = 0$$

with

$$\begin{aligned}
c_4 &= \left(\frac{\omega}{c}\right)^2 \varepsilon_{zz} \\
c_3 &= 2k_\parallel \left(\frac{\omega}{c}\right)^2 \varepsilon_{xz} \\
c_2 &= k_\parallel^2\left(\frac{\omega}{c}\right)^2(\varepsilon_{xx}+\varepsilon_{zz}) + \left(\frac{\omega}{c}\right)^4(\varepsilon_{xz}^2 - \varepsilon_{xx}\varepsilon_{zz} + \varepsilon_{yz}^2 - \varepsilon_{yy}\varepsilon_{zz}) \\
c_1 &= 2k_\parallel^3\left(\frac{\omega}{c}\right)^2 \varepsilon_{xz} + 2k_\parallel\left(\frac{\omega}{c}\right)^4(\varepsilon_{xy}\varepsilon_{yz} - \varepsilon_{xz}\varepsilon_{yy}) \\
c_0 &= \left(\frac{\omega}{c}\right)^6 \det|\varepsilon_{i,j}| + k_\parallel^2\left(\frac{\omega}{c}\right)^4(\varepsilon_{xz}^2 - \varepsilon_{xx}\varepsilon_{zz} + \varepsilon_{xy}^2 - \varepsilon_{xx}\varepsilon_{yy}) + \left(\frac{\omega}{c}\right)^2 k_\parallel^4 \varepsilon_{xx}
\end{aligned} \tag{3}$$

and ξ_λ the eigen vector of the matrix $M(k_\perp^\lambda)_{i,j}$. The transfer matrix for the normal modes of the electric field within layer n is then given by:

$$\begin{pmatrix} E_1^n \\ E_2^n \\ E_3^n \\ E_4^n \end{pmatrix}(0) = \begin{pmatrix} e^{ik_\perp^{n,1}d^n} & & & \\ & e^{ik_\perp^{n,2}d^n} & & \\ & & e^{ik_\perp^{n,3}d^n} & \\ & & & e^{ik_\perp^{n,4}d^n} \end{pmatrix} \begin{pmatrix} E_1^n \\ E_2^n \\ E_3^n \\ E_4^n \end{pmatrix}(d^n) =: P^n(d^n) \begin{pmatrix} E_1^n \\ E_2^n \\ E_3^n \\ E_4^n \end{pmatrix}(d^n) \tag{4}$$

with d^n the thickness of layer n. The interface transfer matrix at the interface beween two layers is given by the continuity conditions of the magnetic field, the parallel components of the electric fields E_x, E_y, and the dielectric displacement D_z perpendicular to the interface. The equations may be numerically solved by a least square procedure leading to the equation:

$$(\mathbf{f}_\lambda^n \cdot \mathbf{f}_\mu^n) E_\mu^n = (\mathbf{f}_\lambda^n \cdot \mathbf{f}_\mu^{n+1}) E_\mu^{n+1} \tag{5}$$

with

$$\mathbf{f}_\lambda^n = \left(\xi_{\lambda,x}^n, \xi_{\lambda,y}^n, \sum_j \left(\frac{\omega}{c}\right)^2 \varepsilon_{zj} \xi_{\lambda,j}^n, (k^{n,\lambda} \times \xi_\lambda^n)_x, (k^{n,\lambda} \times \xi_\lambda^n)_y, (k^{n,\lambda} \times \xi_\lambda^n)_z \right) \tag{6}$$

and where the scalar product is defined by

$$(\mathbf{f} \cdot \mathbf{g}) := f_1 g_1 + f_2 g_2 + \frac{f_3 g_3}{((\omega/c)^4 \det|\varepsilon_{i,j}^n| \det|\varepsilon_{i,j}^{n+1}|)^{1/3}} + \frac{f_4 g_4 + f_5 g_5 + f_6 g_6}{((\omega/c)^4 \det|\varepsilon_{i,j}^n| \det|\varepsilon_{i,j}^{n+1}|)^{1/6}} \tag{7}$$

Inversion of equation (5) leads to

$$E_\mu^n = (\mathbf{f}^n \cdot \mathbf{f}^n)_{\mu\nu}^{-1} (\mathbf{f}^n \cdot \mathbf{f}^{n+1})_{\nu\lambda} E_\lambda^{n+1} =: Q_{\mu\lambda}^{n,n+1} E_\lambda^{n+1} \tag{8}$$

Having determined the transfer matrices $Q_{\mu\lambda}^{n,n+1}$ and $P^n(d^n)$ we can determine the reflection coefficient for a incident wave given by the components E_1^1, E_2^1 of the first layer using

$$r = \left| \frac{E_1^1 \xi_1^1 + E_2^1 \xi_2^1}{E_3^1 \xi_3^1 + E_4^1 \xi_4^1} \right|^2 \tag{9}$$

and by solving the equation:

$$\begin{pmatrix} E_1^1 \\ E_2^1 \\ E_3^1 \\ E_4^1 \end{pmatrix} = \mathbf{Q}^{1,2} \mathbf{P}^2(d^2) \mathbf{Q}^{2,3} \cdots \mathbf{Q}^{l-1,l} \begin{pmatrix} E_1^l \\ E_2^l \\ 0 \\ 0 \end{pmatrix} \tag{10}$$

where we assume the multilayer system to contain l different layers.

The model used to describe the experimental data is based on the assumption that the dielectric tensor, when expressed in the coordinate system of the LC-molecule, is independent of any external field. Thus the dielectric tensor in the laboratory system is only changed by external electric fields because of the induced rotation of the LC-molecule with respect to the coordinate system of the laboratory. The transformation from the molecular coordinate system to the laboratory system may be described by three Euler angles $(\theta_1, \phi, \theta_2)$ and thus

$$\varepsilon^{Lab} = \mathbf{R}_z^t(\theta_1) \mathbf{R}^t(\phi) \mathbf{R}_z^t(\theta_2) \varepsilon^{LC} \mathbf{R}_z(\theta_1) \mathbf{R}(\phi) \mathbf{R}_z(\theta_2) \tag{11}$$

With $\mathbf{R}_z(\theta_1)\mathbf{R}(\phi)\mathbf{R}_z(\theta_2)$ being rotation matrices around the (z, x, z)-axis respectively. The dielectric tensor ε^{LC} in the molecular coordinate system is assumed to be diagonal with real components $\varepsilon_{11}, \varepsilon_{22}, \varepsilon_{33}$. The reflectivity depends on the dielectric tensor of the laboratory system and thus

$$r = r(\theta_1, \phi, \theta_2) \tag{12}$$

In the presence of a modulated external field,

$$\mathbf{E}^{ext} = \begin{pmatrix} 0 \\ 0 \\ E^{\text{ext}} \end{pmatrix} \cos(\Omega t) \tag{13}$$

we expect $(\theta_1, \phi, \theta_2)$ to be time-dependent with the same period, $\Omega = 2\pi F$, F being the modulation frequency:

$$r = r(\theta_1(t), \phi(t), \theta_2(t)) \tag{14}$$

Using the lock-in amplifier, we measure the first two Fourier coefficients of the time dependent reflectivity of equation (14):

$$r_n := \frac{\Omega}{\pi} \int_0^{2\pi/\Omega} \cos(n\Omega t) \cdot r(\theta_1(t), \phi(t), \theta_2(t))\, dt \tag{15}$$

with $n = 1$ or $n = 2$ (lock-in locked on the modulation frequency or twice this frequency).

Measuring the coefficients r_1 and r_2 as a function of the incident angle of the light beam, we are able to fit the experimental data using time dependent Euler angles, to describe the motion of the molecules.

4. RESULTS AND DISCUSSION

4.1 Determination of Dielectric Constants in Uniaxially Oriented Systems

The SmA phase of the liquid crystal is a uniaxially oriented system. The molecules form a so-called book-shelf structure and the molecular axes are aligned to the rubbing direction.[19,20] As shown in Figure 2a, we defined the x-axis of system to be the rubbing direction, and the z-axis to be the direction normal to the glass plane. The angle of observation, θ_2, is defined as the angle between the x-axis and the plane of incidence. This angle is arbitrarily chosen by rotating the sample cell with respect to the plane of incidence defined by the prism.

If $\theta_2 = 0°$ in the SmA phase, the plane of incidence is coincident with the molecular axis. Considering a refractive index ellipsoid for the liquid crystal layer, one of the principle axes of the ellipsoid coincides with direction of the electric field of light. This means that the optical properties are simply described by the y-component of the diagonal dielectric constant ε_y ($= \varepsilon_{22}$ in this case) for s-light, and by ε_x ($= \varepsilon_{11}$) and ε_z ($= \varepsilon_{33}$) for p-light. Figure 3 shows reflectivities $r(\delta_{ex})$, as a function of the angle of incidence, δ_{ex} observed at 60°C and $\theta_2 = 0°$. The simple optical conditions result in guided wave signals which are a series of clear and sharp dips. This is also the case for $\theta_2 = 90°$ with an interchange of ε_x and ε_y. Comparing these data with theoretical calculations based on the simple Fresnel equation allows us to evaluate the exact thickness of the liquid crystal layer and the diagonal values, $\varepsilon_{11}, \varepsilon_{22}$, and ε_{33} of dielectric tensor in the SmA phase. Figure 3 shows the measured reflectivity data and the theoretical curves calculated with the optical parameters in Table 1.

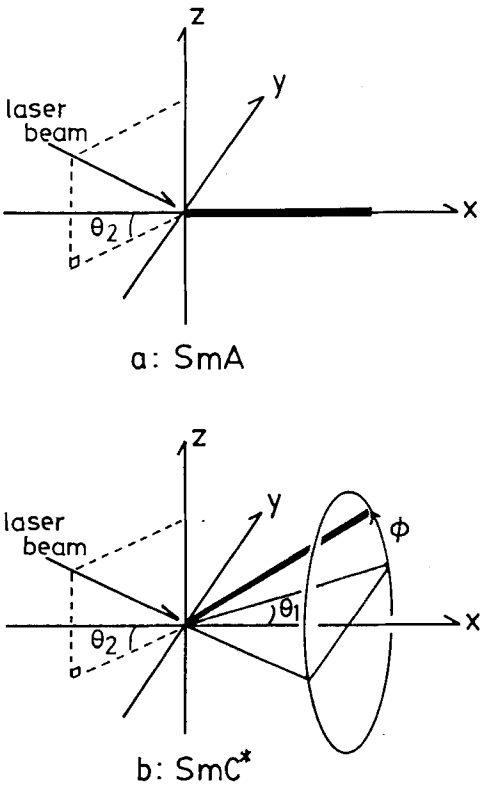

FIGURE 2 Experimental coordinate systems in (a) SmA phase and (b) SmC* phase. The bold lines represent the molecular axis of the liquid crystal molecule.

In the SmC* phase, the molecular axis is tilted by a given angle θ_1 from the x-axis. In order to define the molecular orientation we require the azimuthal angle ϕ as shown in Figure 2b. Choosing these coordinate and angles, θ_1, ϕ, and θ_2, the molecular coordinate can be transformed to the laboratory coordinate system using Euler rotation of Equation 11. Under a sufficiently large external E-field, the angle ϕ is fixed at 0° or 180°, depending on the polarity of E-field, i.e. the molecular axis lies in the x-y plane but at angles $+\theta_1$ or $-\theta_1$ to the x-axis. Since the sign of E-field can be taken arbitrarily, we assigned a $+E$ sign for the case of $+\theta_1$. Therefore, if we set θ_2 at θ_1 or $\theta_1 + 90°$ under the external field, $+E$, the beam propagation direction once again coincides with the principle axis of refractive ellipsoid (see Figure 2b).

Figures 4a and 4b show reflectivity curves in the SmC* phase under E-fields of both polarities, where θ_2 was set to the tilt angle: $\theta_2 = \theta_1 = 25°$. In Figure 4a, where the applied voltage is $+15$V and the thickness 3.56 μm, sharp guided wave modes with no birefringence can be seen. The diagonal dielectric constants of SmC* phase can be determined from the measurements of p- and s-light observed at $\theta_2 = 25°$ and $\theta_2 = 25° + 90°$, using a similar procedure to that for the SmA phase. The optical parameters thus obtained are also listed in Table 1.

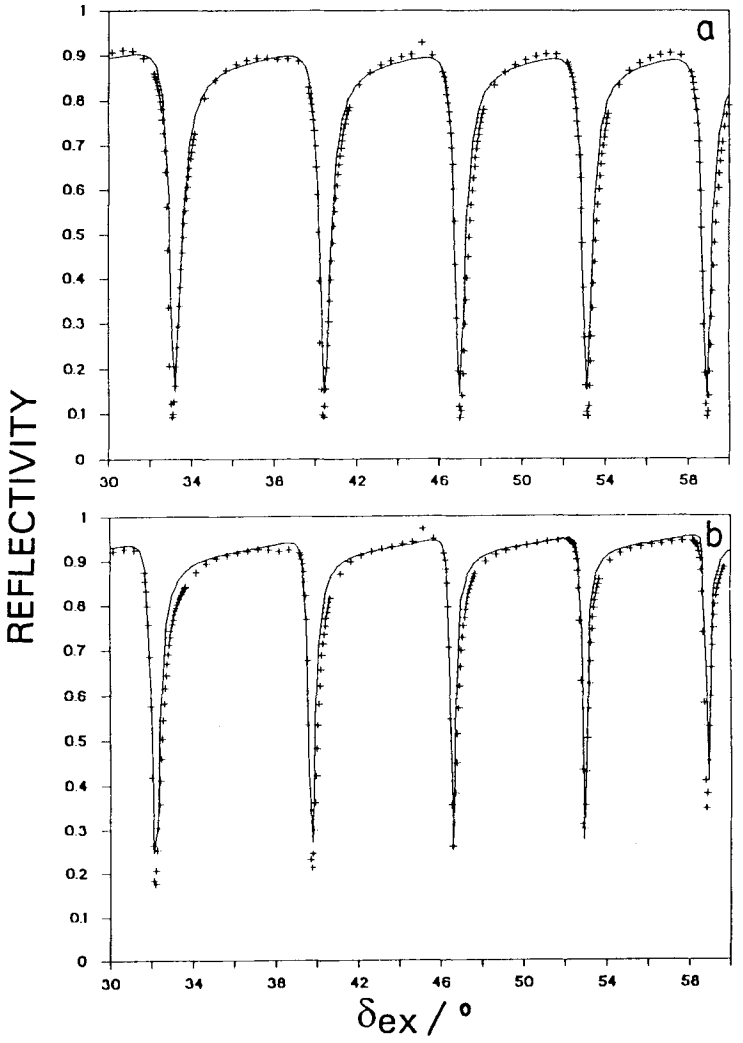

FIGURE 3 Reflectivity of (a) *p*-light and (b) *s*-light as a function of the external angle of incidence δ_{ex}, observed in the SmA phase (60°C) at $\theta_2 = 0°$. The solid lines in (a) and (b) are Fresnel calculations for the angles $\theta_1 = \theta_2 = 0°$ using the parameters of Table I.

TABLE I

Fresnel fitting parameters for the SmA phase (60 °C) and SmC*(52 °C) phase

	glass	gold	polyimide	ε_{11}	LC(SmA) ε_{22} and ε_{33}	ε_{11}	LC(SmC*) ε_{22} and ε_{33}
ε_r^a	2.296	−12.351	2.52	2.57	2.23	2.63	2.22
ε_1^a	0	1.366	0	0	0	0	0
d^b/nm	–	39.9	43.5		3590		3560

[a] real and imaginary parts of the dielectric constant, respectively
[b] thickness of the layer

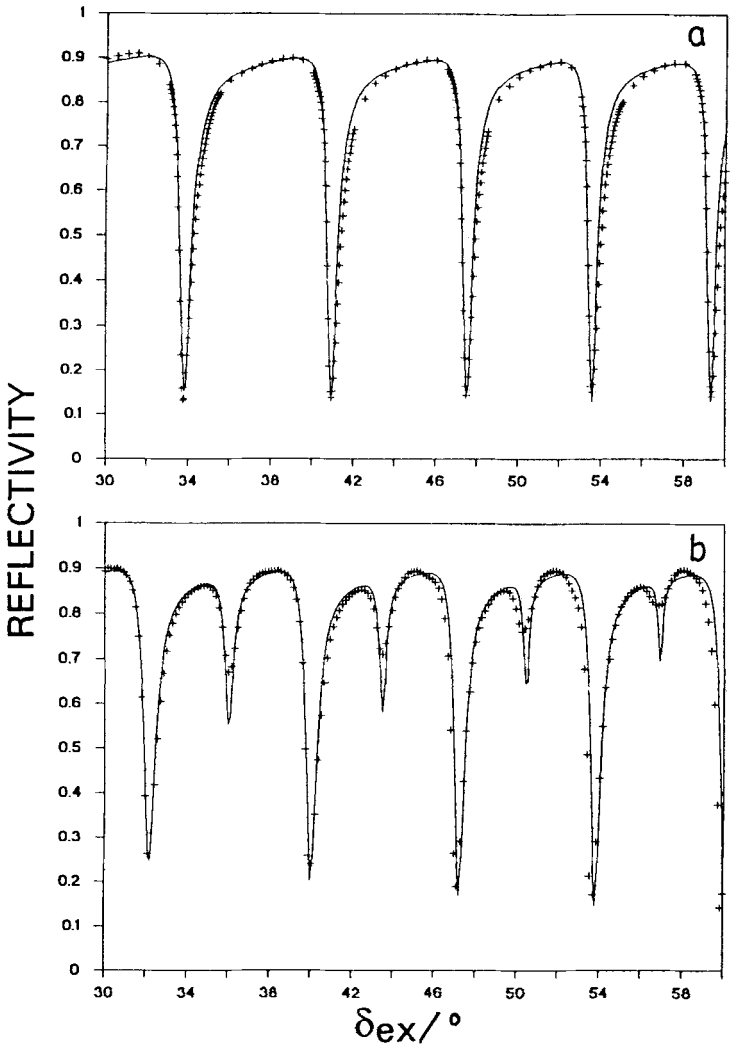

FIGURE 4 Reflectivity of p-light in the SmC* phase (52 °C), observed at $\theta_2 = 25°$. Applied voltages are (a) + 15 V and (b) − 15 V for 3.56 μm thickness, that is, the amplitude of E-field is 4.2×10^4 V/cm. The solid lines are Fresnel fits with $\varepsilon_{11} = 2.625$, $\varepsilon_{22} = 2.224, \varepsilon_{33} = 2.224$, and the angles between the plane of incidence and the molecular axis are taken to be (a) 0° and (b) 47°.

It is known that a chevron layer structure is generally formed in the SmC* phase when the layer thickness decreases, and the formation has been observed by X-ray diffraction.[21] Sambles *et al.*, applied guided waves for probing the chevron layer structure and evaluated the profile of tilt angles as a function of layer distance from the substrates.[11–16] They showed that, when the director is tilted of the plane of incidence, there is strong optical coupling between *p*- and *s*-light, which results in additional dips

on the reflectivity curve such as the data in Figure 4b. However, if a large external E-field is applied, the molecules tend to align perpendicular to the direction of E-field which deforms the system to a quasi-bookshelf structure. Sato *et al.* directly observed by X-ray diffraction that the layer structure changes from the chevron structure to a quasi-bookshelf structure by applying an AC electric field.[22] As shown in Figure 4a, a series of sharp dips on the reflectivity curve without birefringence effect indicate that the SmC* structure is well described as a uniaxially oriented system, which means that the structure under the large E-field can be regarded as a quasi-bookshelf structure.

4.2 Birefringent Systems

An E-field of opposite (negative) polarity induces a strong birefringence effect on the reflectivity curve as shown in Figure 4b, because the direction of beam propagation is different from the principle axes of the ellipsoid. The molecules are forced to take another azimuthal angle $\phi = 180°$, so the axis must be nearly on the x-y plane, and is tilted ca. $50°$ $(= 2\theta_1)$ from the plane of incidence. This situation is confirmed by a theoretical analysis of the reflectivity, $r(\theta_1, \phi, \theta_2)$ using Equation 12: considering the Euler rotation of Equation 11, the reflectivity $r(25°, 180°, 25°)$ is equal to $r(-25°, 0°, 25°)$. The solid line in Figure 4b is calculated using the same optical parameters as those of Figure 4a, but the angles $(\theta_1, \phi, \theta_2)$ were changed from $(25°, 0°, 25°)$ to $(-22°, 0°, 25°)$, this means that the molecular axis is tilted to the plane of incidence by 47°. Thus, the guided wave measurements allow us to probe the molecular swing induced by the external E-field.

Alternating E-field induces modulation of reflectivity which is sensitively detected by a lock-in apparatus. The signal was fed into the lock-in amplifier and treated with the reference frequency of the applied AC field. Figure 5 shows the contrast in reflectivity, $r_1(\delta_{ex})$ (single frequency modulation signal) as a function of δ_{ex}. r_1 is theoretically given by Equation 15 and $n = 1$. The applied modulating E-field has a maximum amplitude of 4.2×10^4 V/cm and a frequency $F = 1$ kHz. Under such a low frequency, a sinusoidal E-field does not result in sinusoidal response in the molecular orientation, since the molecule remains at angle θ_1 until a threshold E-field is reached. Since the molecular response at the threshold is fast compared to the alternating E-field, the modulated response is rectangular, and thus the modulation signal of reflected intensity in Figure 5 is approximately given by the difference of reflectivities, $r(+E)$ and $r(-E)$ in Figures 4a and 4b, which were measured under static E-fields, $+E$ and $-E$, respectively,

$$r_1 = r(+E) - r(-E) \tag{16}$$

The theoretical line in Figure 5 also exhibits a good fit to the observed data, i.e. we can predict the switching behavior using Euler rotation of θ_1 and ϕ, choosing a suitable observation angle θ_2.

4.3 Transient Analysis of the Switching Motion

Because of the threshold behavior, the modulation signal r_1 is given by the difference between two reflectivities corresponding to the equilibrium positions of molecular axes, which are depicted with bold lines in Figure 6. Our interest in this section is focussed on

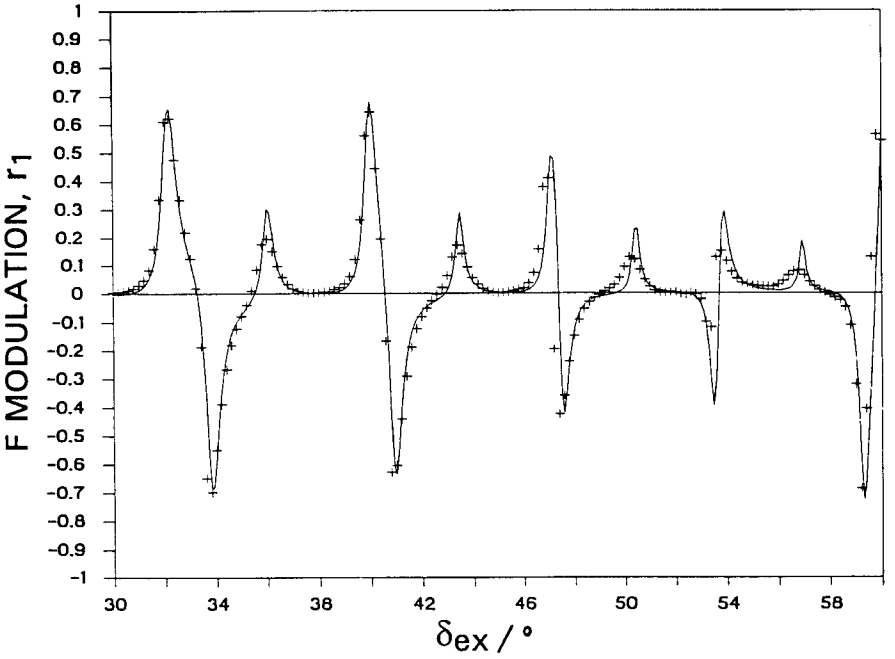

FIGURE 5 F modulation signal r_1 for p-light as a function of the angle of incidence δ_{ex}, observed at $\theta_2 = 25°$. The applied E-field is 1 kHz, 4.2×10^4 V/cm at the maximum of the sinusoidal wave. The solid line is a theoretical calculation with the same parameters as in Figure 4.

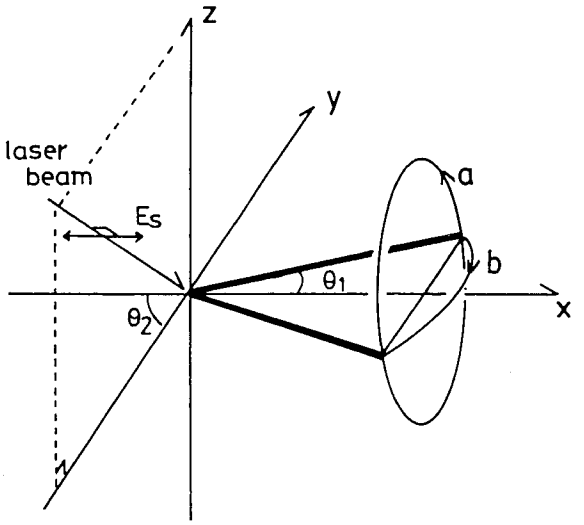

FIGURE 6 Schematic drawing of the coordinate system and the presumed route of the switching motion.

the path of the molecular swing. We try to differentiate between two possible routes: a) goldstone mode rotation around the x-axis (out of plane motion on the cone) and b) soft mode rotation around z-axis (in-plane motion), as depicted in Figure 6. Preliminary calculations using the theory indicated that the most sensitive optical configuration to distinguish between these paths is incident s-light at $\theta_2 = 90°$. As shown in Figure 6, the direction of electric field of the propagating light, E_s, lies in the x-axis. The x-axis is now the symmetrical axis of the molecular motion. In principle, there should be no signal with frequency F, since the optically symmetrical location of the two equilibrium states gives us the same reflected intensities at any δ_{ex}'s, that is, the modulation signal given by the difference of the intensities should be zero. For the sake of a better understanding, an example of oscillograms for the applied voltage and the reflectivities is schematically dipicted in Figure 7. The symmetrical arrangement provides the same amplitude of reflectivity both for the positive and negative E-fields. In reality, however, it is hard to locate the precisely symmetrical position and to adjust the angle θ_2 to be exactly 90° within an error less than one degree. We usually got large r_1 signals on the lock-in amplifier, because of a slightly asymmetrical positioning of the sample and of the high sensitivity of lock-in apparatus to the tiny modulation of reflectivity. Figure 8 shows the $r_1(\delta_{ex})$ data observed with an alternating E-field of 3×10^4 V/cm at 1 kHz. The calculation, the solid line in Figure 8, easily reproduces this result using the angle $\theta_2 = 91°$, i.e. the error of positioning was 1°.

At the midpoint of the switching motion, the system should show reflectivities corresponding to the rotated positions of the molecular axis, which, of course, differ

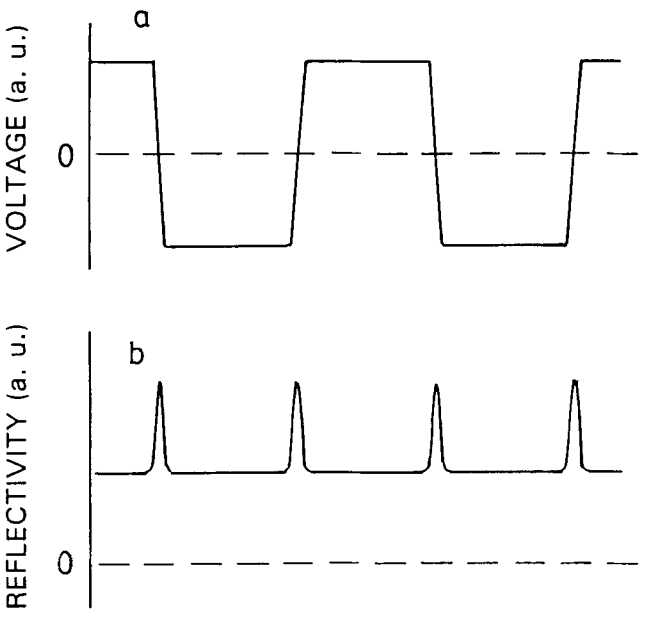

FIGURE 7 Schematic drawing of oscillograms observed at a symmetrical arrangement of optical axes: (a) applied AC voltage and (b) reflectivity.

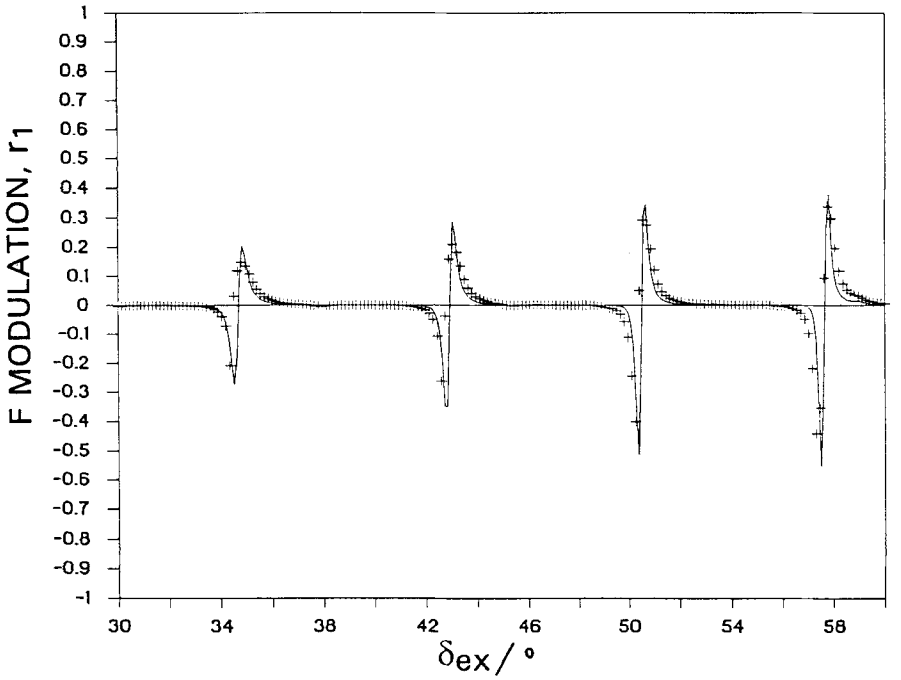

FIGURE 8 F modulation signal r_1 for s-light under an alternating square wave E-field of 1 kHz, 3×10^4 V/cm. The solid line is calculated with the following parameters: $\varepsilon_{11} = 2.630, \varepsilon_{22} = 2.224, \varepsilon_{33} = 2.224$, $d = 3.470\,\mu$m, $\theta_1 = 25°$ and $\theta_2 = 91°$.

from the equilibrium states. Carefully observed, the oscillogram in Figure 7 shows this transient phenomenon as a spike of the reflectivity signal between the positive and negative E-fields. This deviation is recorded as a double frequency signal r_2 on the lock-in amplifier, since the switching takes place twice, i.e., back and forth, during one period T of the E-field alternation. The observed $2F$ signals, $r_2(\delta_{ex})$, are plotted in Figure 9. We calculated the reflectivities for a lot of midpoints of the route a) and route b) of Figure 6, using the time dependent Euler angles plotted in Figures 10a and 10b. The time dependence takes care of the bistability of the two equilibrium positions and we use the switching time τ, for the molecule to switch from one equilibrium position to the other, as a fit parameter for the r_2 modulation signal. The reflectivities were calculated in steps of 10° of ϕ for path a) and 5° of θ_1 for path b), interpolated, and numerically integrated via Equation 15. Theoretical predictions for route a) and route b) are drawn with solid lines in Figures 9a and 9b, respectively. These figures clearly show that the molecule takes the route a) in Figure 6 with a switching time $\tau = 30\,\mu s = 0.03T$, i.e. a goldstone mode on a cone of 25° around the x-axis. Thus, the use of double frequency signals on a lock-in apparatus allows us selective detection of transient orientation of molecules on the course of switching motion.

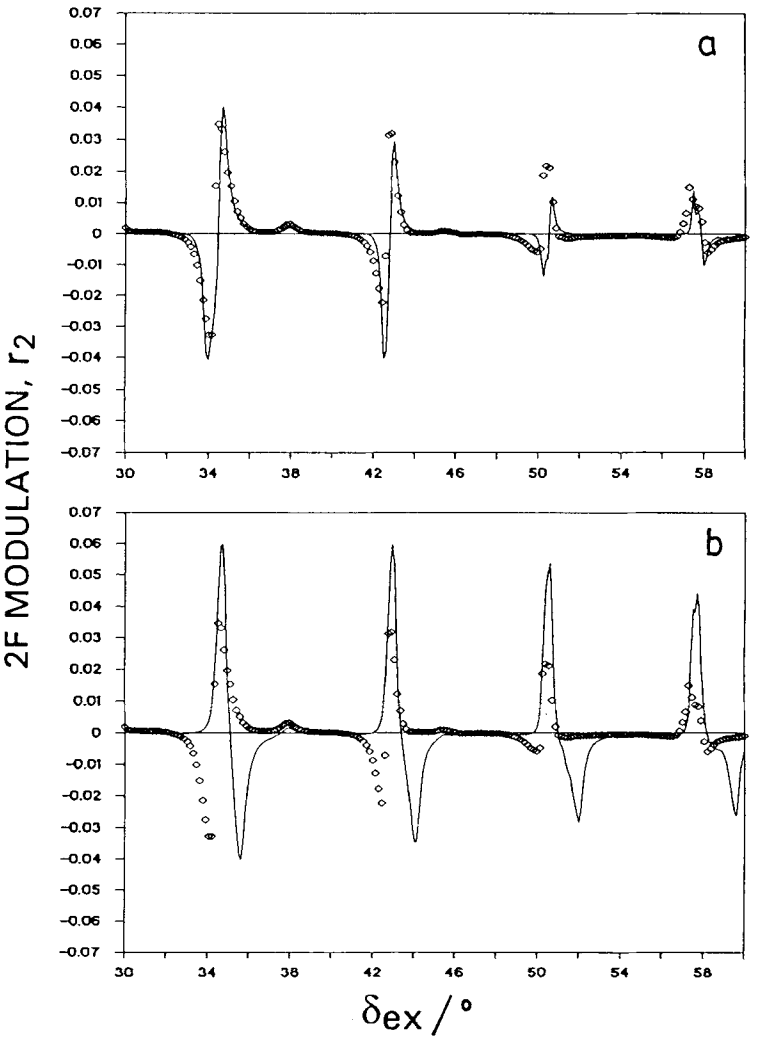

FIGURE 9 Observed double frequency ($2F$) signals r_2 and theoretical calculations for (a) route a) and (b) route b) in Figure 6. The solid lines are calculated with $\tau = 30\,\mu s$ and the same parameters as in Figure 8.

Finally this guided wave method should be compared with other techniques, especially with the time-resolved FT-IR spectroscopy which is a powerful technique for probing field induced reorientation of the liquid crystal molecules.[23,24] It is possible to observe the rotation of IR-active segments through the time-dependent absorption of polarized IR light. One of the particular advantages of IR spectroscopy lies in the capability of seeing individual segment composing the liquid crystal molecule. But, polarization of the probe light often suffers from the birefringence effect of the medium. On the other hand, the waveguide method analyzes the birefringence itself, caused by the rotation of dielectric tensor.

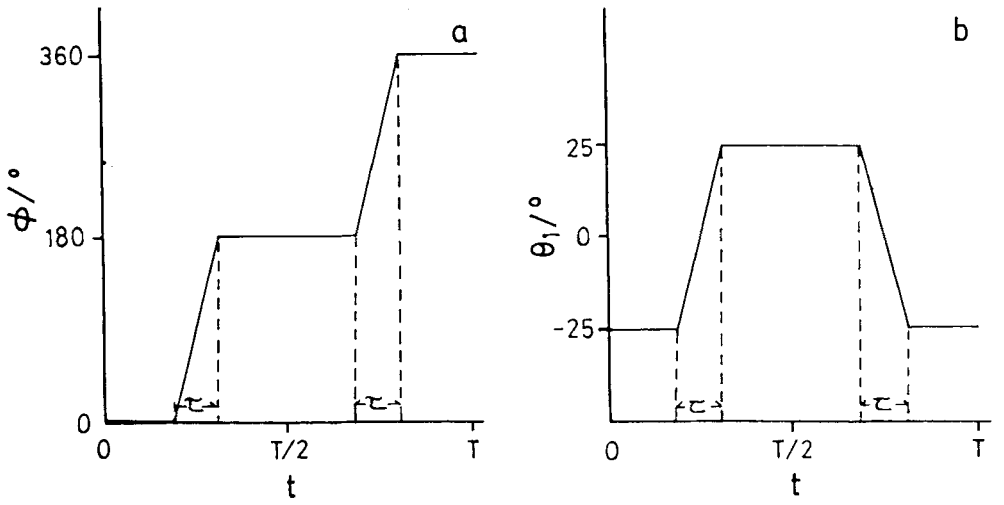

FIGURE 10 Time dependent Euler angles during one period T of the alternating E-field: (a) route a) and (b) route b) in Figure 6.

5. CONCLUSION

A birefringence analysis of guided waves was performed in order to evaluate the optical parameters of a ferroelectric liquid crystal layer. The resonance conditions were described by the layer thickness, by three diagonal elements of dielectric tensor and by Euler angles transforming from the liquid crystal to the laboratory coordinate system. All quantities were successfully determined by the use of both p- and s-polarized light for the guided waves, and by choosing suitable observation angles with respect to the direction of molecular axis. The calculations gave us insight into the orientation and movement of the molecules, by modelling the rotation of refractive index ellipsoid in the three dimensional space. Compared with polarization microscope measurements, guided waves are a more sensitive system for the detection of quantities normal to the plane of the layer and are, of course, able to measure dynamic changes of these quantities on the time scale of microseconds. We have demonstrated the use of guided waves for these systems and expect that this technique should make possible the measurement of interesting liquid crystal effects, e.g., molecular dynamics at the phase transition and the influence of surface constraints on this.

Acknowledgements

The authors are grateful to A. Schönfeld for dielectric measurements of liquid crystals, and to M. Liley for helpful discussions. This work is partly supported by the CIBA-GEIGY foundation, Japan, for the Promotion of Science. S. Ito would like to thank the Max-Planck-Gesellschaft for providing a fellowship.

References

1. P. K. Tien, *Rev. Mod. Phys.*, **49**, 361 (1977).
2. W. Knoll, *Makromol. Chem.*, **192**, 2827 (1991).
3. W. Knoll, *MRS Bulletin*, **16** (7), 29 (1991).
4. W. Hickel and W. Knoll, *Appl. Phys. Lett.*, **57**, 1286 (1990).
5. D. Hornauer and H. Raether, *Optics Commun.*, **7**, 297 (1973).
6. B. Alberti and I. R. Peterson, *Makromol. Chem. Makromol. Symp.*, **46**, 415 (1991).
7. S. Lagerwall, B. Otterholm and K. Skarp, *Mol. Cryst. Liq. Cryst.*, **152**, 503 (1987).
8. R. B. Meyer, *Mol. Cryst. Liq. Cryst.*, **40**, 33 (1977).
9. N. A. Clark and S. T. Lagerwall, *Appl. Phys. Lett.*, **36**, 899 (1980).
10. K. R. Welford, J. R. Sambles and M. G. Clark, *Liquid Crystals*, **2**, 91 (1987).
11. S. J. Elston, *Liquid Crystals*, **9**, 769 (1991).
12. S. J. Elston and J. R. Sambles, *Appl. Phys. Lett.*, **58**, 1381 (1991).
13. S. J. Elston and J. R. Sambles, *Mol. Cryst. Liq. Cryst.*, **200**, 167 (1991).
14. C. A. Lavers, P. S. Cann, J. R. Sambles and E. P. Raynes, *J. Modern Optics*, **38**, 451 (1991).
15. F. Yang and J. R. Sambles, *J. Opt. Soc. Am. B*, **10**, 858 (1993).
16. G. P. Bryan-Brown, J. R. Sambles and K. R. Welford, *J. Appl. Phys.*, **73**, 3603 (1993).
17. S. Ito, F. Kremer, E. Aust and W. Knoll, *J. Appl. Phys.*, **75** 1962 (1994).
18. D. W. Berreman, *J. Opt. Soc. Am.*, **62**, 502 (1972).
19. K. Yoshino, M. Ozaki, S. Kishio, T. Sakurai, N. Mikami, R. Higuchi and M. Honma, *Mol. Cryst. Liq. Cryst.*, **144**, 87 (1987).
20. S. U. Vallerien, F. Kremer, H. Kapitza, R. Zentel and W. Frank, *Phys. Lett. A*, **138**, 219 (1989).
21. T. P. Rieker, N. A. Clark, G. S. Smith, D. S. Parmar, E. B. Sirota and C. R. Safinya *Phys. Rev. Lett.*, **59**, 2658 (1987).
22. Y. Sato, T. Tanaka, H. Kobayashi, K. Aoki, H. Watanabe, H. Takeshita, Y. Ouchi, H. Takezoe and A. Fukuda, *Jpn. J. Appl. Phys.*, **28**, L483 (1989).
23. K. Nito, H. Takanashi and A. Yasuda, *Proceedings of 4th International Conference on Ferroelectric Liquid Crystals*, 383 (1993).
24. H. Sugiswa, H. Toriumi and H. Watanabe, *Mol. Cryst. Liq. Cryst.*, **214**, 11 (1992).